A Journal of the Gesellschaft Deutscher Chemiker

Angewandte International Edition Chemie

GDCh

www.angewandte.org

Accepted Article

Title: Spontaneous α-C-H Carboxylation of Ketones by Gaseous CO2 at the Air-water Interface of Aqueous Microdroplets

Authors: Pallab Basuri, Sinchan Mukhopadhyay, K. S. S. V. Prasad Reddy, Keerthana Unni, B. K. Spoorthi, Jenifer Shantha Kumar, Sharma S. R. K. C. Yamijala, and Thalappil Pradeep

To be cited as: *Angew. Chem. Int. Ed.* **2024**, e202403229

Link to VoR: https://doi.org/10.1002/anie.202403229

WILEY VCH

10.1002/anie.202403229

WILEY VCH

COMMUNICATION

Spontaneous α-C-H Carboxylation of Ketones by Gaseous CO_2 at the Air-water Interface of Aqueous Microdroplets

Pallab Basuri,‡[a] Sinchan Mukhopadhyay,‡ [a] K. S. S. V. Prasad Reddy,[b] Keerthana Unni,[a] B. K. Spoorthi,[a] Jenifer Shantha Kumar,[a] Sharma S. R. K. C. Yamijala,[c] and Thalappil Pradeep*[a]

[a] Pallab Basuri, Sinchan Mukhopadhyay, Keerthana Unni, B. K. Spoorthi, Jenifer Shantha Kumar, and Thalappil Pradeep
DST Unit of Nanoscience and Thematic Unit of Excellence, Department of Chemistry
Indian Institute of Technology Madras
Chennai, Tamil Nadu, India, 600036
E-mail: pradeep@iitm.ac.in

[b] K. S. S. V. Prasad Reddy
Department of Chemistry
Indian Institute of Technology Madras
Chennai, Tamil Nadu, India, 600036

[C] Sharma S. R. K. C. Yamijala
Centre for Atomistic Modelling and Materials Design, Centre for Molecular Materials and Functions, Centre for Quantum Information, Communication, and Computing, Department of Chemistry
Indian Institute of Technology Madras
Chennai, Tamil Nadu, India, 600036

‡ These authors contributed equally to this work

Supporting information for this article is given via a link at the end of the document.

Abstract: We present a catalyst-free route for the reduction of carbon dioxide integrated with the formation of a carbon-carbon bond at the air/water interface of negatively charged aqueous microdroplets, at ambient temperature. The reactions proceed through carbanion generation at the α-carbon of a ketone followed by nucleophilic addition to CO_2. Online mass spectrometry reveals that the product is an α-ketoacid. Several factors, such as the concentration of the reagents, pressure of CO_2 gas, and distance traveled by the droplets, control the kinetics of the reaction. Theoretical calculations suggest that water in the microdroplets facilitates this unusual chemistry. Furthermore, such a microdroplet strategy has been extended to seven different ketones. This work demonstrates a green pathway for the reduction of CO_2 to useful carboxylated organic products.

Increasing carbon dioxide emissions in the atmosphere and decreasing forest cover of Earth are some of the biggest concerns of humanity. CO_2 capture and conversion are methods to tackle this problem. Researchers worldwide have come up with several plausible solutions that include capturing CO_2 by advanced materials,[1] reducing it by electrochemical means,[2] and converting it to small organic molecules.[3][4] Among these, a direct chemical reaction between CO_2 and organic molecules to form fine chemicals is particularly advantageous from an industrial point of view. However, direct nucleophilic addition by a carbanion to the C-center of the chemically inert CO_2 to form a carbon-carbon bond is energetically unfavorable. To overcome this, much attention was given to catalytic processes such as electrochemical[2,5] and photoelectrochemical[6,7] reduction of CO_2, photocatalytic artificial photosynthesis,[8,9] and catalytic reduction.[10,11] However, most of the processes are complex, energy-consuming, expensive, and environmentally unfriendly in totality. Therefore, we need simple, ecofriendly, and efficient methods to convert CO_2 into value-added products.

Microdroplets are promising platforms for understanding chemical and biological reactions occurring at small volumes, single cells, and at single-molecule levels. They exhibit an extraordinary physicochemical environment in comparison to conventional synthesis in bulk solutions. For example, enormous enhancement in the rate of the reaction,[12] spontaneous reduction of species,[13,14] and occurrence of unfavorable reactions,[15,16][17] are known in microdroplets. Recently, we found that the high acidity of microdroplets protonates carboxylic acids to make them electrophiles to undergo nucleophilic addition-elimination reaction.[18] Similarly, Huang et al. showed that microdroplets could protonate inert CO_2 (g) at the gas-liquid interface followed by a reaction with aliphatic amines forming a C-N bond.[19] This

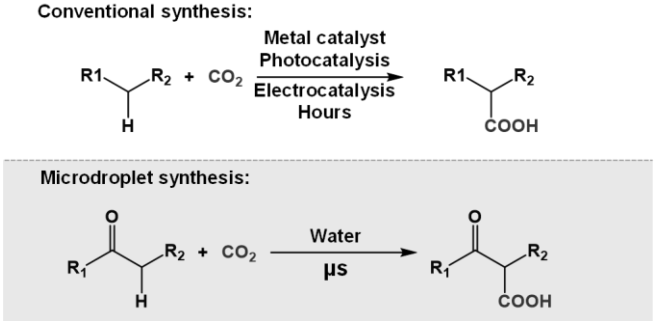

Scheme 1. A comparative study of CO_2 to C-C bond formation using conventional method[20–25] vs microdroplet method.

10.1002/anie.202403229

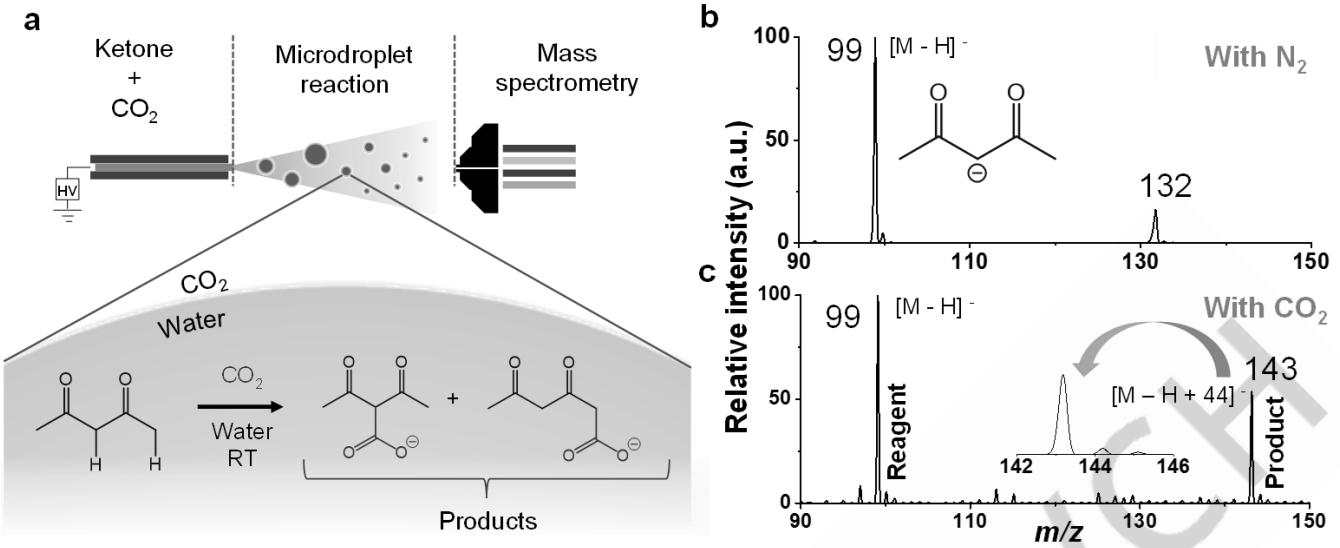

Figure 1. Microdroplet reaction between acetylacetone and CO_2(g). a) Schematic illustration of experimental procedure and scheme of reaction between acetylacetone and CO_2. CO_2 can exist in solution too, in addition to the interface, as it dissolves in water. Mass spectrum of 10 mM acetylacetone in water in b) nitrogen and c) CO_2-nebulized electrospray. Inset of b shows structure of the species detected corresponding to AcAc anion. Inset of c shows the zoomed-in spectrum of the peak at *m/z* 143.

reaction shows tremendous acceleration using carbonate and bicarbonate salts.[26] The Zare group recently found that aqueous microdroplets containing 1,2,3-triazole can efficiently convert CO_2 into formic acid.[27] They have further demonstrated a reaction between toluene and CO_2 in water microdroplets.[28] Ge et al. has also demonstrated that the gas-liquid interface of microdroplets significantly accelerates photocatalytic CO_2 reduction reactions.[29][30]

Here, we utilized the unique environment of microdroplets to achieve CO_2 reduction in-water integrated with C-C bond formation, leading to carboxylation at the α-position of an aliphatic ketone. Online mass spectrometry was performed to characterize the reaction.

Scheme 1 compares the CO_2 reduction toward C-C coupling performed using the slow conventional bulk synthesis methods[20–25] with the rapid microdroplet synthesis. Figure 1 shows the results from microdroplet reaction of acetylacetone (AcAc) with CO_2(g). The detailed experimental protocol is presented in Supporting Information 1. The reaction was carried out by performing electrospray of AcAc (aq.) in negative ion mode in a nebulized condition at 5 µL/min flow rate and -3 kV spray voltage, as shown in Figure 1a. In N_2-nebulized electrospray ionization, the major species seen was deprotonated AcAc $[M - H]^-$ at *m/z* 99 (Figure 1b), further confirmed by its collision induced dissociation, resulting in a fragmented peak at *m/z* 57 (neutral loss of CH_2CO) as shown in Figure S1a. Strikingly, by changing the nebulization gas from N_2 to CO_2, a product peak at *m/z* 143, $[M - H + 44]^-$, was seen (Figure 1c). The conversion ratio (CR), the ratio between the product and reagent plus product intensities expressed in percentage, i.e., CR (%) = $[I_P / (I_P + I_R)] \times 100$, was 35%. Tandem mass spectrometry of the product peak at *m/z* 143 gave two major fragmented species corresponding to CO_2 and H_2O losses, and two minor peaks due to CO and C_2H_6 losses, respectively (Figure S1b). MS/MS/MS of the isolated peak at *m/z* 99 again showed a characteristic loss of CH_2CO (Figure S1c) which matched with the MS/MS of AcAc. Scheme S1 shows structures of the major fragmented species. The loss of CO_2 requires a moderate collision energy (~40 V) as evident from Figure S2. All of these give us confidence to identify the peak to be a covalently bonded product of a reaction between the ketone and CO_2. Among the two positional isomeric products in Figure 1a, we speculate that the carboxylation reaction occurs at the center position of AcAc, due to the higher acidity of these two protons compared to the protons in the methyl groups. The product peak was further confirmed by performing the droplet reaction with an isotopically labeled reagent (Figure S3). Note that we did not observe any di-carboxylated product, as evident from the MS/MS spectrum of the peak at *m/z* 187 (Figure S4), which arises from the background. We also conducted a bulk reaction by continuous bubbling of CO_2 in a solution of AcAc. A time-dependent ESI MS measurement of the bulk reaction mixture shows no product formation (SI 2 and Figure S5). To rule out any possibility of contamination from the experimental setup, we recorded background spectra that showed complete absence of the reagent or product (Figure S6).

We then performed pressure dependent experiment to evaluate the effect of CO_2 concentration at the droplet interface. Figure S7 shows the CR vs. CO_2 gas pressure plot. To our surprise, we observed a drastic decay of the CR with increasing nebulization gas pressure. With increasing gas pressure, the concentration of CO_2 around the droplet environment cannot be significantly increased. Although, the actual concentration of CO_2 around the droplet is hard to evaluate. We believe that within the lowest pressure regime, the CO_2 concentration around the droplet is significantly higher that it reaches the saturation limit of the reaction. In this case, we suggest that the droplet velocity plays convert into product, hence, high CR.[28] Similar results were also

10.1002/anie.202403229

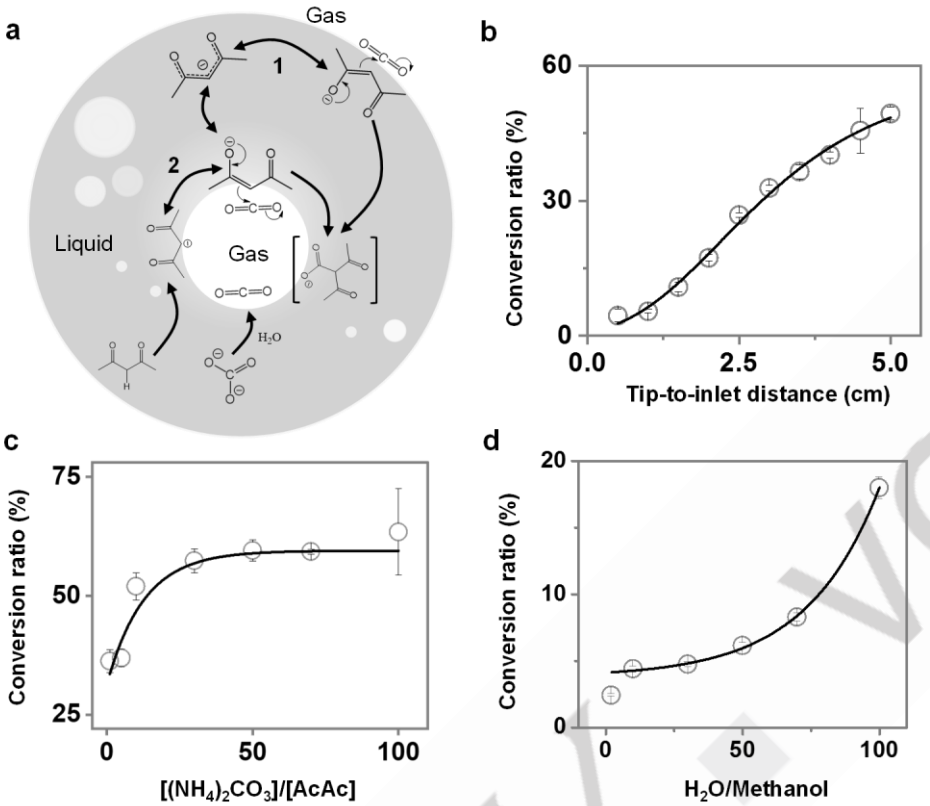

Figure 2. Microdroplet reaction at different conditions. a) In-droplet carboxylation reaction mechanism involving both intrinsic formation of CO_2 from the dissociation of ammonium carbonate and externally nebulized CO_2. Effect of b) tip-to-inlet distance, c) ratio of ammonium carbonate and acetylacetone and d) ratio of water and methanol on the reaction progression.

observed in the distance experiments, discussed later in this article.

The concentrations of the reactants are indeed an important parameter in controlling the rate of the reaction in such microdroplet chemistry.[31] We observed a dramatic concentration effect when we varied the concentration of AcAc from 1 µM to 10 mM. Figure S8a displays a stack of mass spectra at different concentrations. We found that the product peak intensity falls exponentially with increasing the reagent concentration, as shown in Figure S8b. At low concentration, most of the AcAc anions are available at the surface to participate in reaction with CO_2, in contrast to the high concentration where molecules at the droplet core are unreactive, lowering down the overall CR.

The spray potential has been found to have a minimal effect on the conversion ratio (Figure S9a). Upon increasing it from 0 to 1.5 kV, ionization efficiency increases which drives the reaction. Note that at 0 kV, we only observe a noise (Figure S9b). We believe that AcAc ion concentration saturates at 1.5 kV spray potential resulting in a plateau in the potential vs CR plot of the reaction.

We then planned a different approach for the reaction and used $(NH_4)_2CO_3$ as a source of CO_2. By spraying 1:30 molar ratio of AcAc:$(NH_4)_2CO_3$ in water, we observed a deprotonated species corresponding to carboxylation of AcAc (Figure S10). We also observed a significant increase in the product peak intensity in this case than in the CO_2-nebulization experiment. The CR was ~75%. We also performed a reaction with CO_2 present in ambient air which resulted in low product yield as compared to that from a gas cylinder (Figure S11).

Contrary to the observation by Cooks et al., where the authors reported C-N bond formation with CO_2 and amine, both in positive and negative ion modes, we found no reaction in the positive ion mode. A peak at *m/z* 145 was observed at low intensity in the positive ion mode, although the MS/MS spectrum did not show a characteristic neutral loss of CO_2 (Figure S12). We speculate that the mechanism (Figure 2a) of the reaction involves the formation of carbanion nucleophiles in the first place in negatively charged microdroplets. This is due to the high acidity of the enolate proton, which undergoes C-H cleavage to make the carbanion. Such negatively charged species occupy the gas-liquid interface to minimize the electrostatic repulsion and cause nucleophilic attack to the C-center of the CO_2. For CO_2 nebulized conditions, the microdroplet surface acts as a reaction site, as shown by reaction path 1 (Figure 2a). However, the reaction with ammonium carbonate undergoes via its decomposition to CO_2(g) which eventually creates micro/nano-bubbles at the interior of the droplet as shown in Figure 2a. Gas-liquid interfaces of such micro/nano-bubbles serve as a reaction site for this heterogenic interfacial reaction (path 2). Such nanobubbles within microdroplets have been observed previously.[32] Notably, reaction via dissolved CO_2 in water cannot be overruled both in CO_2 nebulization and with ammonium carbonate. We excluded any electrochemical pathway of the reaction through radical generation by performing a control experiment with the addition of TEMPO which does not affect our reaction (Figure S13).

10.1002/anie.202403229

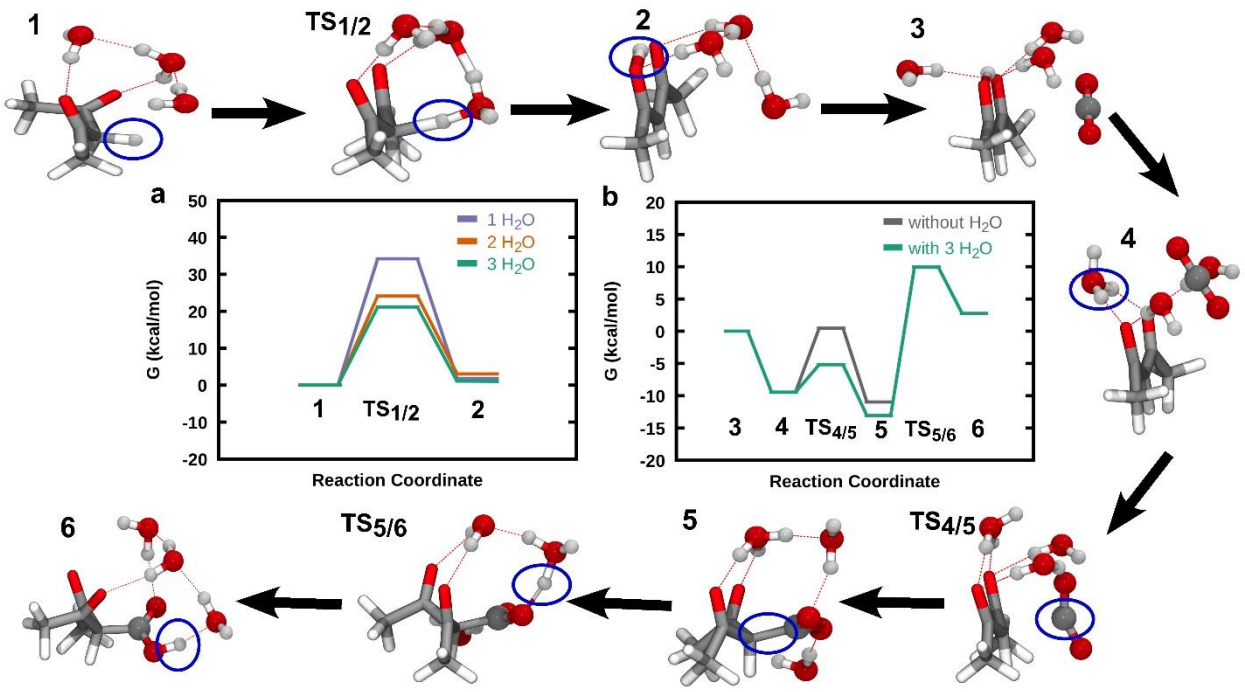

Figure 3. Free energy landscape for CO_2 reduction over AcAc and DFT optimized structures in the presence of three explicit water molecules along the reaction pathway.

Tip-to-inlet distance is known to affect microdroplet chemistry by regulating the flight time of the droplets. We observed a dramatic difference in the CR by changing the tip-to-inlet distance. Figure 2b shows a sigmoidal increase of the CR with increasing distance from 0.5 to 5 cm while spraying AcAc with $(NH_4)_2CO_3$. This suggests that the reaction progression depends highly on the time travelled by the droplet in air**.** Figure S14 shows a series of mass spectra with varying distances. A similar experiment with CO_2 nebulization was performed (Figure S15). We observed that beyond a distance of 3 cm, the CR decreases which might be due to complete desolvation resulting in the release of the gas phase ion. To account for the droplet size effect, we have conducted a control experiment in which we varied the tip diameter of the emitter while maintaining a constant distance of 1.5 cm. We found that reducing the tip diameter increases the product peak intensity significantly (Figure S16). The smaller the droplets higher the surface area. It proves that the reaction is occurring at the surface of the droplet. This contributes to the enrichment of the reactant molecules at the surface, resulting in an increased conversion ratio.[33]

Encouraged by the above findings, we performed an experiment by varying the $(NH_4)_2CO_3$ to AcAc ratio in solution. In Figure 2c we found that the CR rises quickly from 10 to 70% by increasing the $(NH_4)_2CO_3$ ratio from 5 to 30%. After that, it reaches a plateau. Mass spectra of the corresponding ratios are shown in Figure S17. Additionally, we performed imaging experiments of deposited droplets to visualize the number of microbubbles formed (Figure S18a-c). We observed that the number density of microbubbles per droplet increases significantly with increasing the concentration of $(NH_4)_2CO_3$ (Figure S18d).

We found that the reaction is not supported by organic solvents. To check the effect of organic solvents, we added methanol to the bulk solution. By varying the solvent composition from 0% to 95% of H_2O in methanol, we found an increase of CR from 3 to 18% at a 1:1 molar ratio of the ammonium carbonate to AcAc (Figure 2d). Figure S19 shows the mass spectra of the corresponding data points at different solvent compositions. Firstly, we assessed that owing to high dielectric constant, water in the droplet helps in holding the net charges better than the organic contents such as methanol. Which in turn drives the generation of the carbanion to react with CO_2 at the interface. Secondly, we suggest that this could also be regulated by the equilibrium of ammonium carbonate to CO_2 conversion. At higher water concentrations, the equilibrium shifts to the CO_2 side which helps in generating microbubbles for the reaction to occur.

We further verified our conjecture of reaction through microbubbles by changing the pH of the solution. We observed that lowering the pH of the solution linearly increases the CR of the reaction (Figure S20). We concluded that low pH influences the formation of microbubbles inside microdroplets.

To understand the effect of ionic strength, we conducted an experiment by adding a noninteractive salt, $CaCl_2$ and compared the results with the results in the absence of it (Figure S21). Interestingly, we observed a significant increment of product peak intensity upon the addition of $CaCl_2$. The addition of non-interactive salt is known to influence the reaction rate when the reaction proceeds through the formation of a charged species. The increase of product peak intensity upon the addition of $CaCl_2$ further supports our mechanism that the reaction goes through the formation of the carbanion. The addition of $CaCl_2$ will induce an increased concentration of Cl^- ions in the droplet. We assessed that an increased concentration of Cl^- ions increases the rate of the reaction. Thus, we observed an increased conversion ratio after the addition of $CaCl_2$.

10.1002/anie.202403229

To gain deeper insights into the reduction mechanism of CO_2 in the presence of AcAc and water, we conducted a series of density functional theory simulations (see computational details for further details) on the complexes of AcAc, CO_2, and H_2O. We examined the role of solvent molecules by varying the number of explicit water molecules in our simulations from one to three and found that the presence of explicit water molecules plays a crucial role in capturing CO_2. The CO_2 reduction reaction begins with the formation of a carbanion complex from AcAc through the keto-enol tautomerism. The Gibbs free energy profiles for the tautomerism with varying numbers of explicit water molecules are shown in Figure 3(a). Complex 1 represents AcAc solvated with three explicit water molecules. The proton transfer (keto-enol tautomerism) within AcAc generates complex 2, and the transition state is represented by TS1/2. In the presence of one explicit water molecule, the activation barrier for the proton transfer is about 34.2 kcal/mol, and it is reduced to 21.47 kcal/mol in presence of three explicit water molecules. The drastic decrement in the activation barrier with an increase in the water molecules is due to the ease of proton transfer in the network of more explicit water molecules. The calculated free energy change (ΔG) between the keto and enol tautomer is about 1 kcal/mol, where we find that the keto form is more stable than the enol form. Water, being a polar solvent, slightly stabilizes the keto form with a high dipole moment.[34–37]

Next, we computed the barriers for CO_2 capture using the enol form (complex 2) in three explicit water molecules. The Gibbs free energy profile for this reaction is shown in Figure 3(b). Here, complex 3 depicts the interaction of CO_2 with complex 2 with some reorientation. The transfer of a proton from complex 3 to the surrounding water molecules is exergonic and stabilizes the formation of carbanion complex 4 by -9.45 kcal/mol. The formation of a C-C bond between carbanion (complex 4) and CO_2 generates the carboxylate anion (complex 5). The computed activation barrier for the C-C bond formation is 4.27 kcal/mol. The formation of C-C bond decreases the free energy of the complex 5 to -13.06 kcal/mol. Here, C-C bond distance decreases from 3.75 to 1.6 Å. We also calculated the activation barrier of C-C bond formation between the carbanion and CO_2 in the gas phase, which is 8.9 kcal/mol (Figure 3(b)). Hence, we conclude that CO_2 reduction is facilitated by solvated water. Finally, the transfer of proton from the water molecules to the COO group results in the formation of the carboxylic acid (Complex 6). The barrier for this proton transfer (TS5/6) is around 23 kcal/mol. Complex 6 is less stable than complex 5 since holding a proton on the carboxylate anion is less preferred than releasing it into the water (in other words, carboxylic acid prefers to lose a proton in water). We have also observed a similar result with complex 2, where it was stabilized by approximately 7 kcal/mol by releasing the proton to water (see Figure S22).

We calculated the activation barriers for the formation of a C–C bond in both neutral (i.e., representing the core of the droplet) and charged media (representing the surface of the microdroplet) by considering up to three explicit water molecules. As shown in Figure S23, the barriers for the C–C bond formation in the neutral medium is 19.3 kcal/mol when three explicit water molecules are considered (18.60 and 17.60 kcal/mol in the presence of one and two water molecules, respectively). In contrast, the barrier is only 4.27 kcal/mol when the system is negatively charged. Moreover, for the system representing the microdroplet environment, the carboxylate complex formation step (5) is exergonic, whereas the same step is endergonic for the system representing the bulk environment. Together, these results strongly indicate that the formation of a C–C bond (which is the crucial step in our reaction) is more favorable in microdroplets than in bulk water.

We extended our microdroplet chemistry to several other ketones. These include acetone, 1,1,1-trifluoro-5,5-dimethyl-2,4-hexanedione, benzophenone, acetophenone, dimedone (5,5-dimethylcyclohexane-1,3-dione), and cyclopentane-1,3-dione. Based on the above observations, we decided to perform these reactions with ammonium carbonate with a 1:1 ratio of both the reagents in solution. The mass spectrum and the MS/MS of the reagents and the products are presented in Figures S24-29. The CR values of other products range from 0.008 to 28%, while that for the reaction between 1:1 AcAc and $(NH_4)_2CO_3$ was highest at 33%. Strikingly, we observed that two of the cyclic diketones, i.e., dimedone and cyclopentane-1,3-dione did not react well. We assessed that the reaction mechanism goes through the formation of carbanion from the enol form of the diketones. In the case of AcAc, the keto-enol equilibrium shifts towards the enol side due to the intermolecular hydrogen bonding through a six-member ring formation (as shown below in scheme S2a). However, these two cyclic ketones cannot form stable enol due to their ring strain. The schemes S2b and S2c below show the equilibrium structure of the keto and enol form of the two cyclic diketones. Note that ketones having no α-H do not undergo this reaction (Figure S26). This also supports our reaction mechanism of the formation of carbanion via C-H bond cleavage in charged microdroplets. Our product, β-diketo acid, is known for its instability at room temperature.[38][39] It was also evident from the ESI MS of the crude product where we observed low product yield, synthesized upon two-hour deposition and liquid phase extraction from a scaled-up multiplexed electrospray setup (Figure S30).

In summary, we introduced a method of forming C-C bond with chemically inert CO_2 and the α-carbon of ketones, in charged aqueous microdroplets. Ionization of ketone by a C-H cleavage at the α position is the first step of the reaction. Interfacial enrichment of the newly formed carbanion helps in reaction progression via a nucleophilic attack to the C-center of CO_2, which is a key step of the reaction. Our work shows a tremendous possibility to convert environmental CO_2 to useful products. The science discussed here has implications in understanding interfacial chemistry at the gas-liquid phase, the latter in a confined volume, such as in clouds, aerosols, rain droplets, and mist.

Supporting Information

A brief discussion on the experimental procedures, computational details, MS of the reaction by varying gas pressure, distance, concentration, and solvent effect, MS of the bulk reaction, and MS and MS/MS of other reactants and products, presented in

10.1002/anie.202403229

supporting information. The authors have cited additional references within the Supporting Information.[40–42]

Acknowledgements

P.B. thanks IIT Madras for research fellowship. S.M., K.U., and B.K.S. thank UGC for their research fellowship. T.P. acknowledges funding from the Centre of Excellence on Molecular Materials and Functions under the Institute of Eminence scheme of IIT Madras. S.S.R.K.C.Y. acknowledges the financial support of IIT Madras through the MPHASIS faculty fellowship and through its new faculty support grants NFSG (IP2021/0972CY/NFSC008973), NFIG (RF2021/0577CY/NFIG008973), and DST-SERB (SRG/2021/001455).

Keywords: Carbon dioxide reduction • microdroplet chemistry • air-water interface • mass spectrometry • carbanion

[1] C. Lu, X. Zhang, X. Chen, *Accounts Mater. Res.* **2022**, *3*, 913–921.
[2] S. Nitopi, E. Bertheussen, S. B. Scott, X. Liu, A. K. Engstfeld, S. Horch, B. Seger, I. E. L. Stephens, K. Chan, C. Hahn, J. K. Nørskov, T. F. Jaramillo, I. Chorkendorff, *Chem. Rev.* **2019**, *119*, 7610–7672.
[3] Q. Liu, L. Wu, R. Jackstell, M. Beller, *Nat. Commun.* **2015**, *6*, 5933.
[4] S. Saini, R. S. Das, A. Kumar, S. L. Jain, *ACS Catal.* **2022**, *12*, 4978–4989.
[5] T. N. Nguyen, M. Salehi, Q. Van Le, A. Seifitokaldani, C. T. Dinh, *ACS Catal.* **2020**, *10*, 10068–10095.
[6] V. Kumaravel, J. Bartlett, S. C. Pillai, *ACS Energy Lett.* **2020**, *5*, 486–519.
[7] A. U. Pawar, C. W. Kim, M.-T. Nguyen-Le, Y. S. Kang, *ACS Sustain. Chem. Eng.* **2019**, *7*, 7431–7455.
[8] J. He, C. Janáky, *ACS Energy Lett.* **2020**, *5*, 1996–2014.
[9] S. R. Lingampalli, M. M. Ayyub, C. N. R. Rao, *ACS Omega* **2017**, *2*, 2740–2748.
[10] A. Modak, P. Bhanja, S. Dutta, B. Chowdhury, A. Bhaumik, *Green Chem.* **2020**, *22*, 4002–4033.
[11] M. D. Porosoff, J. G. Chen, *J. Catal.* **2013**, *301*, 30–37.
[12] Z. Wei, Y. Li, R. G. Cooks, X. Yan, *Annu. Rev. Phys. Chem.* **2020**, *71*, 31–51.
[13] J. K. Lee, D. Samanta, H. G. Nam, R. N. Zare, *J. Am. Chem. Soc.* **2019**, *141*, 10585–10589.
[14] J. K. Lee, D. Samanta, H. G. Nam, R. N. Zare, *Nat. Commun.* **2018**, *9*, 1562.
[15] I. Nam, J. K. Lee, H. G. Nam, R. N. Zare, *Proc. Natl. Acad. Sci.* **2017**, *114*, 12396 LP – 12400.
[16] I. Nam, H. G. Nam, R. N. Zare, *Proc. Natl. Acad. Sci.* **2018**, *115*, 36 LP – 40.
[17] A. J. Grooms, A. N. Nordmann, A. K. Badu-Tawiah, *Angew. Chemie Int. Ed.* **2023**, *62*, e202311100.
[18] P. Basuri, L. E. Gonzalez, N. M. Morato, T. Pradeep, R. G. Cooks, *Chem. Sci.* **2020**, *11*, 12686–12694.
[19] K.-H. Huang, Z. Wei, R. G. Cooks, *Chem. Sci.* **2021**, *12*, 2242–2250.
[20] T. Fujihara, Y. Tsuji, *Front. Chem.* **2019**, *7*.
[21] C.-K. Ran, L.-L. Liao, T.-Y. Gao, Y.-Y. Gui, D.-G. Yu, *Curr. Opin. Green Sustain. Chem.* **2021**, *32*, 100525.
[22] W. Huang, J. Lin, F. Deng, H. Zhong, *Asian J. Org. Chem.* **2022**, *11*, e202200220.
[23] A. Banerjee, G. R. Dick, T. Yoshino, M. W. Kanan, *Nature* **2016**, *531*, 215–219.
[24] S. Wang, G. Du, C. Xi, *Org. Biomol. Chem.* **2016**, *14*, 3666–3676.
[25] J. Luo, I. Larrosa, *ChemSusChem* **2017**, *10*, 3317–3332.
[26] L. Feng, X. Yin, S. Tan, C. Li, X. Gong, X. Fang, Y. Pan, *Anal. Chem.* **2021**, *93*, 15775–15784.
[27] X. Song, Y. Meng, R. N. Zare, *J. Am. Chem. Soc.* **2022**, *144*, 16744–16748.
[28] Y. Meng, E. Gnanamani, R. N. Zare, *J. Am. Chem. Soc.* **2023**, *145*, 7724–7728.
[29] Q. Ge, Y. Liu, K. Li, L. Xie, X. Ruan, W. Wang, L. Wang, T. Wang, W. You, L. Zhang, *Angew. Chemie Int. Ed.* **2023**, *62*, e202304189.
[30] Q. Ge, Y. Liu, W. You, W. Wang, K. Li, X. Ruan, L. Xie, T. Wang, L. Zhang, *PNAS Nexus* **2023**, *2*, pgad389.
[31] C. J. Chen, E. R. Williams, *Chem. Sci.* **2023**, *14*, 4704–4713.
[32] P. Basuri, A. Chakraborty, T. Ahuja, B. Mondal, J. S. Kumar, T. Pradeep, *Chem. Sci.* **2022**, *13*, 13321–13329.
[33] B. M. Marsh, K. Iyer, R. G. Cooks, *J. Am. Soc. Mass Spectrom.* **2019**, *30*, 2022–2030.
[34] P. Roy, S. Biswas, A. Pramanik, P. Sarkar, *Int. J. Res. Soc. Nat. Sci* **2017**, *2*, 2455–5916.
[35] J. W. Bunting, J. P. Kanter, R. Nelander, Z. Wu, *Can. J. Chem.* **1995**, *73*, 1305–1311.
[36] T. Tsukahara, K. Nagaoka, K. Morikawa, K. Mawatari, T. Kitamori, *J. Phys. Chem. B* **2015**, *119*, 14750–14755.
[37] G. Alagona, C. Ghio, P. I. Nagy, *Phys. Chem. Chem. Phys.* **2010**, *12*, 10173–10188.
[38] K. J. Pedersen, *J. Am. Chem. Soc.* **1929**, *51*, 2098–2107.
[39] A. V Ignatchenko, M. E. Springer, J. D. Walker, W. W. Brennessel, *J. Phys. Chem. C* **2021**, *125*, 3368–3384.
[40] J.-D. Chai, M. Head-Gordon, *Phys. Chem. Chem. Phys.* **2008**, *10*, 6615–6620.
[41] M. J. Frisch, G. W. Trucks, H. B. Schlegel, G. E. Scuseria, M. A. Robb, J. R. Cheeseman, G. Scalmani, V. Barone, G. A. Petersson, H. Nakatsuji, *Google Sch. There is no Corresp. Rec. this Ref.* **2020**.
[42] A. V Marenich, C. J. Cramer, D. G. Truhlar, *J. Phys. Chem. B* **2009**, *113*, 6378–6396.

10.1002/anie.202403229

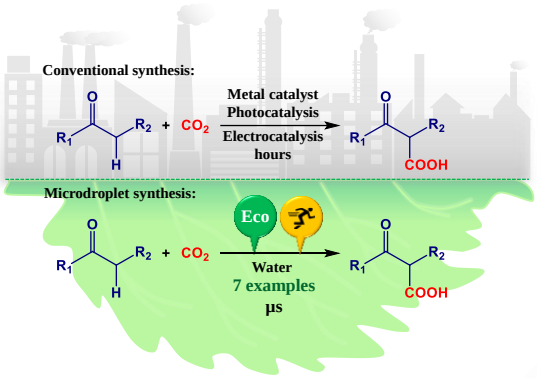

Charged aqueous microdroplets facilitate carboxylation at α-C-H position of ketones by gaseous CO_2 at the air-water Interface.